Superheavy nuclei in a relativistic effective Lagrangian model

Tapas Sil,[1] S. K. Patra,[2] B. K. Sharma,[2] M. Centelles,[1] and X. Viñas[1]
[1]*Departament d'Estructura i Constituents de la Matèria, Facultat de Física, Universitat de Barcelona, Diagonal 647, 08028 Barcelona, Spain*
[2]*Institute of Physics, Sachivalaya Marg, Bhubaneswar 751 005, India*
(Received 1 October 2003; published 26 April 2004)

Isotopic and isotonic chains of superheavy nuclei are analyzed to search for spherical double shell closures beyond $Z=82$ and $N=126$ within the new effective field theory model of Furnstahl, Serot, and Tang for the relativistic nuclear many-body problem. We take into account several indicators to identify the occurrence of possible shell closures, such as two-nucleon separation energies, two-nucleon shell gaps, average pairing gaps, and the shell correction energy. The effective Lagrangian model predicts $N=172$ and $Z=120$ and $N=258$ and $Z=120$ as spherical doubly magic superheavy nuclei, whereas $N=184$ and $Z=114$ show some magic character depending on the parameter set. The magicity of a particular neutron (proton) number in the analyzed mass region is found to depend on the number of protons (neutrons) present in the nucleus.

DOI: 10.1103/PhysRevC.69.044315 PACS number(s): 21.60.−n, 21.10.Dr, 21.30.Fe, 27.90.+b

I. INTRODUCTION

In the last thirty years a continuing effort has been devoted to the investigation of superheavy nuclei both in experiments and in theoretical research. A fascinating challenge in the study of these nuclei is the quest for the islands of stability where the next magic numbers beyond $N=126$ and $Z=82$ may be located. Experiments made at GSI, Dubna and Berkeley have allowed the synthesis and detection of some superheavy nuclei. For instance, light isotopes of the elements $Z=110$, 111, and 112 have been obtained at GSI and Dubna [1–3]. They have been identified by their characteristic α-decay chains which lead to already known isotopes. These new nuclei are expected to be deformed, consistently with the predicted occurrence of a deformed magic shell closure at $Z=108$ and $N=162$ (see, e.g., Refs. [4–6]). First data of some heavier and more neutron-rich isotopes of atomic number $Z=112$ ($N=171$), $Z=114$ ($N=173-175$), and $Z=116$ ($N=176$) produced by means of fusion reactions have also been measured at Dubna [7].

Theoretical predictions made at the end of the sixties pointed towards the existence of an island of long-lived superheavy elements (SHE) centered around $N=184$ and $Z=114$ [8–11]. The nuclei around the hypothetical doubly magic element $^{298}114$ were expected to be nearly spherical with longer half-lives. Such superheavy nuclei, having a negligible liquid-drop fission barrier, would be stabilized mostly by quantal shell effects. Many of the more recent theoretical works on superheavy nuclei are based on the nuclear mean field approach and can be classified in two main groups. On the one hand, we have the macroscopic-microscopic models which include a liquid-drop contribution for the part of the energy which varies smoothly with the number A of nucleons, and a shell correction contribution obtained from a suitable single-particle potential for the fine tuning. On the other hand, there are the self-consistent Hartree-Fock or Hartree calculations based on Skyrme forces or on the relativistic nonlinear $\sigma-\omega$ model, respectively.

The nuclei in the range around $Z\approx 110$ already detected in experiments bridge the gap between the known actinides and the unknown superheavy elements. With the advent of more experimental data, a commendable endeavor has been undertaken in nuclear structure research [6,12–25] aimed at verifying the reliability of the present theoretical models in the regime of the heavier actinides and of the discovered superheavy nuclei around $Z=110$, which requires deformed calculations. The fact that many of the observed data for SHE are for odd-even decay chains renders the calculations and the comparison with experiment even more complicated, since the deformed level density is high and the observed nuclei may be in isomeric states. Calculations with self-consistent models of some α-decay chains [20], deformation energy curves along the fission path [25], and shell structures [6] find that there is a gradual transition from well-deformed nuclei around the deformed $Z=108$ and $N=162$ shell closures to spherical shapes approaching larger superheavy nuclei around the putative $N=184$ magic neutron gap, in qualitative agreement with the earlier studies in mac-mic and semiclassical models. Still, the Hartree-Fock model mass formula of Ref. [26] predicts large deformations in many of the isotopes of $Z=114$ and in almost all of the $Z=120$ isotopes. As pointed out in some recent works, the description of deformed SHE may require to consider triaxial deformations and reflection-asymmetric shapes [25,27,28] (Ref. [29] pioneered the relativistic mean field triaxial calculations). It is even possible that there exist isolated islands of stability associated with exotic (semibubble, bubble, toroidal, and bandlike) topologies in nuclei with very large atomic numbers [20,30,31].

Another long-standing goal of the nuclear structure studies in the field of superheavy nuclei has been to establish the location in N and Z of the next *spherical double* shell closures for elements heavier than ^{208}Pb, and of the largest shell effects which are a necessary condition for the stability of SHE against fission. In this context, most of the calculations published in the literature are performed in spherical symmetry. It is well established that the macroscopic-microscopic calculations predict spherical shell closures at $Z=114$ and $N=184$ [4]. In self-consistent calculations, however, the proton and neutron shell structures strongly affect each other

and other N and Z values can appear as candidates for shell closures depending on the model interaction. For example, Hartree-Fock calculations with a variety of Skyrme forces show the most pronounced spherical shell effects at $Z=124,126$, and $N=184$ [32–36]. As an exception to this rule, Skyrme parametrizations such as SkI3 and SkI4 which have a modified spin-orbit interaction prefer $Z=120$ and $Z=114$, respectively, for the proton shell closure [33,34]. Hartree-Fock-Bogoliubov calculations with the finite range Gogny force predict $Z=120,126$ and $N=172,184$ as possible spherical (or nearly spherical) shell closures [30,31]. At variance with Skyrme Hartre-Fock, the relativistic mean field (RMF) theory with the conventional scalar and vector meson field couplings typically prefers $Z=120$ and $N=172$ as the best candidates for spherical shell closures [32–36]. Of course, the different nature of the spin-orbit interaction in the Skyrme and RMF models is pivotal in deciding the location of the stronger shell effects. Detailed comparisons between Skyrme Hartree-Fock and RMF calculations of SHE can be found in Refs. [33] and [35].

The discrepancies in the predicted spherical shell closures for SHE motivate us to reinvestigate them using the more general RMF model derived from the chiral effective Lagrangian proposed by Furnstahl, Serot, and Tang [37–39]. In this first attempt to apply the effective field theory (EFT) model to the region of superheavy nuclei we will restrict ourselves to analyze the occurrence of double shell closures and the shell stabilizing effect in spherical symmetry, as done, e.g., in Refs. [32–36]. We want to learn whether in this respect the EFT approach shows a different nature compared to the usual RMF theory or not. The possible extension of the calculations to deformed geometries and the subsequent application of the EFT model to the heavier actinides and the lighter transactinides where experimental data have been measured is left for future consideration.

The relativistic model of Refs. [37–39] is a new approach to the nuclear many-body problem which combines the modern concepts of effective field theory and density functional theory (DFT) for hadrons. An EFT assumes that there exist natural scales to a given problem and that the only degrees of freedom relevant for its description are those which can unravel the dynamics at the scale concerned. The unresolved dynamics corresponding to heavier degrees of freedom is encoded in the coupling constants of the theory, which are determined by fitting them to known experimental data. The Lagrangian of Furnstahl, Serot, and Tang is intended as an EFT of low-energy QCD. As such, its main ingredients are the lowest-lying hadronic degrees of freedom and it has to incorporate all the infinite (in general nonrenormalizable) couplings consistent with the underlying symmetries of QCD. To endow the model with predictive power the Lagrangian is expanded and truncated. Terms that contribute at the same level are grouped together with the guidance of naive dimensional analysis. Truncation at a certain order of accuracy is consistent only if the coupling constants eventually exhibit naturalness (i.e., if they are of order unity when in appropriate dimensionless form). In the nuclear structure problem the basic expansion parameters are the ratios of the scalar and vector meson fields and of the Fermi momentum to the nucleon mass M, as these ratios are small in normal situations. To solve the equations of motion that stem from the constructed effective Lagrangian one applies the relativistic mean field approximation in which the meson fields are replaced by their classical expectation values.

EFT and DFT are bridged by interpreting the expansion of the effective Lagrangian as equivalent to an expansion of the energy functional of the many-nucleon system in terms of nucleon densities and auxiliary meson fields. The RMF theory is then viewed as a covariant formulation of DFT in the sense of Kohn and Sham [40]. That is, the mean field model approximates the exact, unknown energy functional of the ground-state densities of the nucleonic system, which includes all higher-order correlations, using powers of auxiliary classical meson fields. This merger of EFT and DFT provides an approach to the nuclear problem which retains the simplicity of solving variational Hartree equations with the bonus that further contributions, at the mean field level or beyond, can be incorporated in a systematic and controlled manner.

If the chiral effective Lagrangian is truncated at fourth order, in mean field approach one recovers the same couplings of the usual nonlinear $\sigma-\omega$ model plus additional nonlinear scalar-vector and vector-vector meson interactions, besides tensor couplings [38,39]. The free parameters of the resulting energy functional have been fitted to ground-state observables of a few doubly magic nuclei. The fits, parameter sets named G1 and G2 [38], do display naturalness and are not dominated by the last terms retained; an evidence which confirms the usefulness of the EFT concepts and validates the truncation of the effective Lagrangian at the first lower orders. The ideas of EFT have been fruitful [41], moreover, to elucidate the empirical success of previous RMF models, like the original $\sigma-\omega$ model of Walecka [42] and its nonlinear extensions with cubic and quartic scalar self-interactions [43]. However, these conventional RMF models truncate the effective Lagrangian at some level without further physical rationale or symmetry arguments. The introduction of new interaction terms in the effective model pursues an improved representation of the relativistic energy functional [38,39].

Previous works have shown that the EFT model is able to describe in a unified manner the properties of nuclear matter, both at normal and at high densities [44,45], as well as the properties of finite nuclei near and far from the valley of β stability [46,47], with similar and even better quality to standard RMF force parameters. With this positive experience at hand, in the present paper we want to investigate the predictability of the new effective Lagrangian approach to the nuclear many-body problem in extrapolations to superheavy nuclei. Concretely, we shall focus on analyzing the model predictions for spherical shell closures. Our calculations will be performed in spherical symmetry. Though deformation is an important degree of freedom for SHE [5,6,14,18,25], we are searching for spherical shell stability around $^{298}_{184}114$ and $^{292}_{172}120$ where deformation is expected to be small and where the shell structure has often been analyzed in the spherical approximation [5,32–36]. For exploration, we also compute hyperheavy nuclei around $N\sim 258$ which spherical calculations have found to correspond to a possible region of increased shell stability [36]. Deformation would certainly

change the picture in the details and add deformed shell closures, e.g., like those predicted around $Z=108$ and $N=162$ [4–6], but it should not change drastically the predictions for the values of N and Z where the strongest shell effects show up already in the spherical calculation. Of course, for a quantitative discussion, one needs to account for deformation effects which will serve to extend the island of shell stabilized superheavy nuclei and to decide on the specific form of the ground-state shapes of these nuclei.

Our analysis uses the EFT parameter sets G1 and G2 [38]. The results are compared with those obtained with the NL3 parameter set [48], taken as one of the best representatives of the usual RMF model with only scalar self-interactions. The paper is organized as follows. In Sec. II we briefly summarize the RMF model derived from EFT and our modified BCS approach to pairing. Section III is devoted to the study of several properties of superheavy nuclei such as two-particle separation energies and shell gaps, average pairing gaps, single-particle energy spectra, and shell corrections. The summary and conclusions are laid in Sec. IV.

II. FORMALISM

A. The model

The EFT model used here has been developed in Ref. [38]. Further insight into the model and the concepts underlying it can be gained from Refs. [37,39,41,49]. For our purposes, the basic ingredient is the EFT energy density functional for finite nuclei. It reads [38,39]

$$\begin{aligned}\mathcal{E}(\mathbf{r}) = \sum_{\alpha} \varphi_{\alpha}^{\dagger}\Bigg\{ & -i\alpha\cdot\boldsymbol{\nabla} + \beta(M-\Phi) + W + \frac{1}{2}\tau_3 R + \frac{1+\tau_3}{2}A \\ & - \frac{i}{2M}\beta\alpha\cdot\left(f_v\boldsymbol{\nabla}W + \frac{1}{2}f_\rho\tau_3\boldsymbol{\nabla}R + \lambda\boldsymbol{\nabla}A\right) + \frac{1}{2M^2}(\beta_s \\ & + \beta_v\tau_3)\Delta A\Bigg\}\varphi_\alpha + \left(\frac{1}{2} + \frac{\kappa_3}{3!}\frac{\Phi}{M} + \frac{\kappa_4}{4!}\frac{\Phi^2}{M^2}\right)\frac{m_s^2}{g_s^2}\Phi^2 \\ & - \frac{\zeta_0}{4!}\frac{1}{g_v^2}W^4 + \frac{1}{2g_s^2}\left(1+\alpha_1\frac{\Phi}{M}\right)(\boldsymbol{\nabla}\Phi)^2 - \frac{1}{2g_v^2}\left(1+\alpha_2\frac{\Phi}{M}\right) \\ & \times(\boldsymbol{\nabla}W)^2 - \frac{1}{2}\left(1+\eta_1\frac{\Phi}{M} + \frac{\eta_2}{2}\frac{\Phi^2}{M^2}\right)\frac{m_v^2}{g_v^2}W^2 - \frac{1}{2g_\rho^2}(\boldsymbol{\nabla}R)^2 \\ & - \frac{1}{2}\left(1+\eta_\rho\frac{\Phi}{M}\right)\frac{m_\rho^2}{g_\rho^2}R^2 - \frac{1}{2e^2}(\boldsymbol{\nabla}A)^2 + \frac{1}{3g_\gamma g_v}A\Delta W \\ & + \frac{1}{g_\gamma g_\rho}A\Delta R. \end{aligned} \tag{1}$$

The coupling constants have been written so that in the present form they should be of order unity according to the naturalness assumption. The index α runs over all occupied nucleon states $\varphi_\alpha(\mathbf{r})$ of the positive energy spectrum. The meson fields are $\Phi \equiv g_s\phi_0(\mathbf{r})$, $W \equiv g_v V_0(\mathbf{r})$, and $R \equiv g_\rho b_0(\mathbf{r})$, and the photon field is $A \equiv eA_0(\mathbf{r})$. Variation of the energy density (1) with respect to $\varphi_\alpha^\dagger$ and the meson fields gives the Dirac equation fulfilled by the nucleons and the Klein-Gordon equations obeyed by the mesons (see Refs. [38,44] for the detailed expressions). We solve the Dirac equation in coordinate space by transforming it into a Schrödinger-like equation.

In this work we shall employ the EFT parameter sets G1 and G2 of Ref. [38] that were fitted by a least-squares optimization procedure to 29 observables (binding energies, charge form factors, and spin-orbit splittings near the Fermi surface) of the nuclei ^{16}O, ^{40}Ca, ^{48}Ca, ^{88}Sr, and ^{208}Pb. A satisfactory feature of the set G2 is that it presents a positive value of κ_4, as opposed to G1 and to most of the successful RMF parametrizations such as NL3. We note that the value of the effective mass at saturation M_∞^*/M in the EFT sets ($\sim$0.65) is somewhat larger than the usual value in the RMF parameter sets ($\sim$0.60), which is due to the presence of the tensor coupling f_v of the ω meson to the nucleon [46,50]. Also, the bulk incompressibility of G1 and G2 is $K=215$ MeV, while the NL3 set has $K=271$ MeV.

B. Pairing

In order to describe open-shell nuclei the pairing correlations have to be explicitly taken into account. The most popular approach for well-bound isotopes has been the BCS method. However, the BCS approximation breaks down for exotic nuclei near the drip lines because it does not treat the coupling to the continuum properly. This difficulty is disposed of either by the nonrelativistic Hartree-Fock-Bogoliubov theory, with Skyrme [51] and Gogny [52] forces, or by the relativistic Hartree-Bogoliubov (RHB) theory [53–56].

Pairing correlations are another important ingredient in the study of superheavy elements. Furthermore, some of the predicted regions of shell stability in superheavy nuclei lie close to the drip point and a suitable treatment is required. Many calculations of SHE have often used a zero-range two-body pairing force $V_{pair}=V_{0,p/n}\delta(\mathbf{r}-\mathbf{r}')$, with adjustable strengths for protons and neutrons (see Refs. [33,35]). A study of SHE using the RHB approach, with the NL-SH parameter set, was carried out in Ref. [57].

To deal with the pairing correlations we use here a simplified prescription which we have previously found to be in acceptable agreement with RHB calculations [46]. The procedure is similar to the one employed for Skyrme forces in Ref. [58]. For each kind of nucleon we assume a constant pairing matrix element G_q, which simulates the zero range of the pairing force, and we include quasibound levels in the BCS calculation as done in Ref. [58]. These levels of positive single-particle energy, retained by their centrifugal barrier (neutrons) or by their centrifugal-plus-Coulomb barrier (protons), mock up the influence of the continuum in the pairing calculation. The wave functions of the considered quasibound levels are mainly localized in the classically allowed region and decrease exponentially outside it. As a consequence, the unphysical nucleon gas which surrounds the nucleus if continuum levels are included in the normal BCS approach is eliminated [46]. We restrict the space of states involved in the pairing correlation to one harmonic oscillator shell above and below the Fermi level, to avoid the unrealistic pairing of highly excited states and to confine the region

of influence of the pairing potential to the vicinity of the Fermi level.

As described in Ref. [46], the solution of the pairing equations allows us to find the average pairing gap Δ_q for each kind of nucleon. We write the pairing matrix elements as $G_q = C_q/A$. We have fixed the constants C_q by looking for the best agreement of our calculation with the known experimental binding energies of Ni and Sn isotopes for neutrons, and of $N=28$ and $N=82$ isotones for protons [46]. The values obtained from these fits are $C_n=21$ MeV and $C_p=22.5$ MeV for the G1 set, $C_n=19$ MeV and $C_p=21$ MeV for the G2 set, and $C_n=20.5$ MeV and $C_p=23$ MeV for the NL3 interaction.

In Ref. [46] we applied this improved BCS approach with the G1 and G2 parametrizations to study one- and two-neutron (proton) separation energies for several chains of isotopes (isotones) from stability to the drip lines. We found a reasonable agreement with the available experimental data, similar to the one obtained using the NL3 set. The analysis showed that the parameters sets based on EFT are able to describe nuclei far from the β-stability valley when a pairing residual interaction is included.

III. RESULTS AND DISCUSSION

Traditionally a large gap in the single-particle spectrum has been interpreted as an indicator of a shell closure, at least for nuclei of atomic number $Z<100$. However, for a large nucleus such as a superheavy element, it may not be sufficient to simply draw the single-particle level scheme and to look for the gaps, due to the complicated structure of the spectrum and the presence of levels with a high degree of degeneracy. Moreover, in a self-consistent calculation, a strong coupling between the neutron and proton shell structure takes place. Therefore, when dealing with SHE it is imperative to look for other quantities to reliably identify the shell closures and magic numbers, apart from the analysis of the single-particle level structure.

Here we shall consider the following observables as indicators for shell closures.

(1) A sudden jump in the two-neutron (two-proton) separation energies of even-even nuclei, defined as

$$S_{2q} = E(N_q - 2) - E(N_q), \tag{2}$$

where N_q is the number of neutrons (protons) in the nucleus for $q=n$ $(q=p)$. A sharp drop in S_{2q} means that a very small amount of energy is required to remove two more nucleons from the remnant of the parent nucleus. Thus, the parent nucleus is more stable which is a character of magicity. This observable is an efficient tool to quantify the shell effect because of the absence of odd-even effects [33].

(2) The size of the gap in the neutron (proton) spectrum is determined by half of the difference in Fermi energy when going from a closed shell nucleus to a nucleus with two additional neutrons (protons). This quantity is very well accounted for by the two-neutron (two-proton) shell gap which is defined as the second difference of the binding energy [32,33]:

$$\begin{aligned}\delta_{2q}(N_q) &= S_{2q}(N_q) - S_{2q}(N_q + 2) \\ &= E(N_q + 2) - 2E(N_q) + E(N_q - 2).\end{aligned} \tag{3}$$

This quantity measures the size of the step found in the two-nucleon separation energy and, therefore, it is strongly peaked at magic shell closures.

(3) The neutron and proton average pairing gaps Δ_q of open-shell nuclei can be related to the odd-even mass difference, from where the empirical law $\Delta \sim 12/\sqrt{A}$ can be derived [59]. However, for closed shell nuclei Δ_q should vanish. Thus, we shall use the vanishing of the average pairing gap obtained from our calculations as another signal for identifying closed shell nuclei.

We next calculate the above observables for the isotopic chain of $Z=120$ and for several isotonic chains, assuming spherical symmetry. We employ the parameter sets G1 and G2 due to the EFT formalism and compare the results with those obtained from the standard RMF parametrization NL3, which is well established as a successful interaction for nuclei at and away from the line of β stability.

It is to be mentioned that the previous indicators correspond to energy differences between neighboring nuclei. However, they do not have a direct connection with the shell corrections which stabilize a given (N,Z) superheavy nucleus against fission [35]. The shell corrections are related to the difference between the nuclear binding energies and the predictions of a liquid-drop model. As a complementary study, after our search for spherical shell closures, we shall analyze the shell corrections for the discussed chains of SHE.

A. Isotopic chain of $Z=120$

We first consider the chain of isotopes with atomic number $Z=120$, which is found as a magic number in recent relativistic mean field calculations of nuclei in the superheavy mass region [32–35]. Figure 1 collects the results obtained with the EFT parameter set G2. The two-neutron separation energies S_{2n} are displayed in the upper panel of this figure. The S_{2n} graph shows a smooth decrease with increasing neutron number N throughout the whole chain except for the sudden jumps after the neutron numbers $N=172$, 184, and 258. These jumps indicate the possible occurrence of a shell closure at these neutron numbers. Using Eq. (3) we calculate the two-nucleon shell gap for neutrons for the same isotopic chain, and present the result in the middle panel of Fig. 1. Sharp peaks in δ_{2n} are found at the same neutron numbers 172, 184, and 258. It is seen that the peaks of $N=172$ and $N=258$ are more marked than the peak of $N=184$. Actually, the height of the peak at $N=184$ is around only one third of that of the peak at $N=172$. One may note that the amplitude of the jumps in δ_{2n} for shell closures is smaller in the SHE region than in the region of normal mass nuclei. This is expected due to the increase of the single-particle level density with increasing mass number. For example, for ^{208}Pb and for the doubly magic isotopes of tin and calcium we find values of δ_{2n} between some 5 and 10 MeV.

The average pairing gap Δ_q is representative of the strength of the pairing correlations. The curve for the neutron pairing gaps, displayed in the bottom panel of Fig. 1, shows

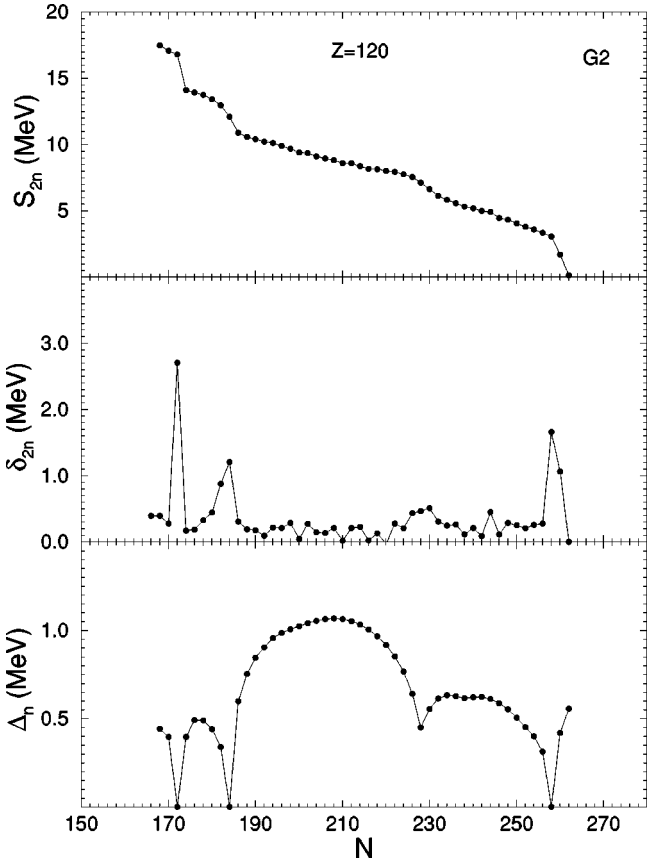

FIG. 1. The change with the neutron number N of the two-neutron separation energy S_{2n}, the two-neutron shell gap δ_{2n}, and the neutron average pairing gap Δ_n for $Z=120$ isotopes obtained from spherical calculations with the relativistic parameter set G2. The proton average pairing gap Δ_p vanishes in the whole isotopic chain.

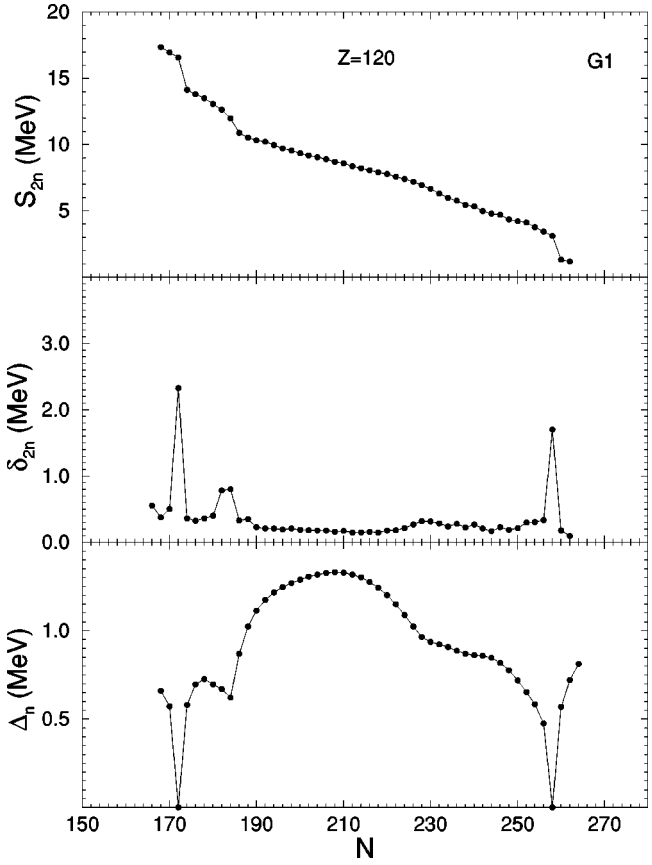

FIG. 2. Same as Fig. 1 but for the relativistic parameter set G1.

a structure of arches that vanish only at $N=172$, 184, and 258. Since the proton pairing gap Δ_p is zero throughout the whole $Z=120$ chain, we have not plotted it. Although we use a simplified prescription for the calculation of the pairing gap [46], our value for Δ_q can be considered as an average of the different state-dependent single-particle gaps which would be obtained if one had used a zero-range pairing force, as done, e.g., in Refs. [33,35].

Therefore, all of the three analyzed observables are pointing to the same neutron numbers as the best candidates for shell closures for $Z=120$ with the G2 parametrization. The magic character of the proton number $Z=120$ in combination with $N=172$, 184, and 258 is tested in the calculations for isotonic chains that we present in the following section. In analyzing the shell effects from a spherical calculation it is to be kept in mind that only for doubly magic nuclei one can guarantee a spherical shape, when protons as well as neutrons experience a spherical shell closure. For open-shell nuclei the spherical solution does not always correspond to the ground state. Inclusion of deformation might add extra stability for some $Z=120$ nuclei other than $^{292}120$, $^{304}120$, and $^{378}120$, and perhaps additional peaks would develop with respect to the neighboring background in the curve for δ_{2n}, apart from the sudden jumps we have detected by means of the spherical calculation. Only a deformed calculation could definitively decide in such cases the appropriate ground-state shape. Nevertheless, the spherical solution gives a first hand and overall view of the sequence of spherical shell closures, which we have obtained from indicators which imply differences of energies but not their absolute values.

In order to analyze the force dependence of the location of the shell closures for the superheavy nuclei, we calculate the quantities S_{2n}, δ_{2n}, and Δ_n with the EFT set G1 and with the NL3 parameter set for the same isotopic chain $Z=120$ and display the results in Fig. 2 and 3, respectively. As in the case of the G2 set, the proton pairing gap Δ_p vanishes for the whole chain of $Z=120$ isotopes and it is not drawn. The global nature of the curves of Figs. 2 and 3 is quite similar to that observed previously with the G2 set. Abrupt jumps in S_{2n} and δ_{2n}, and the vanishing of the average neutron pairing gap Δ_n, indicate shell closures at $N=172$ and 258 in both of the G1 and NL3 sets. The height of the peaks of δ_{2n} at $N=172$ and 258 is very similar between the G1 and G2 sets, while they attain the largest values in the NL3 set. For the $N=184$ system, S_{2n} and δ_{2n} show only a moderate jump in both G1 and NL3, indicating a weaker shell closure than for $N=172$ and 258. Moreover, the neutron pairing gap Δ_n does not vanish at $N=184$ with the G1 and NL3 sets, indicating that the occupancy of the single-particle levels is diffused across the Fermi level, contrarily to the case of G2.

One expects a relatively large energy gap to appear between the last occupied and the first unoccupied single-

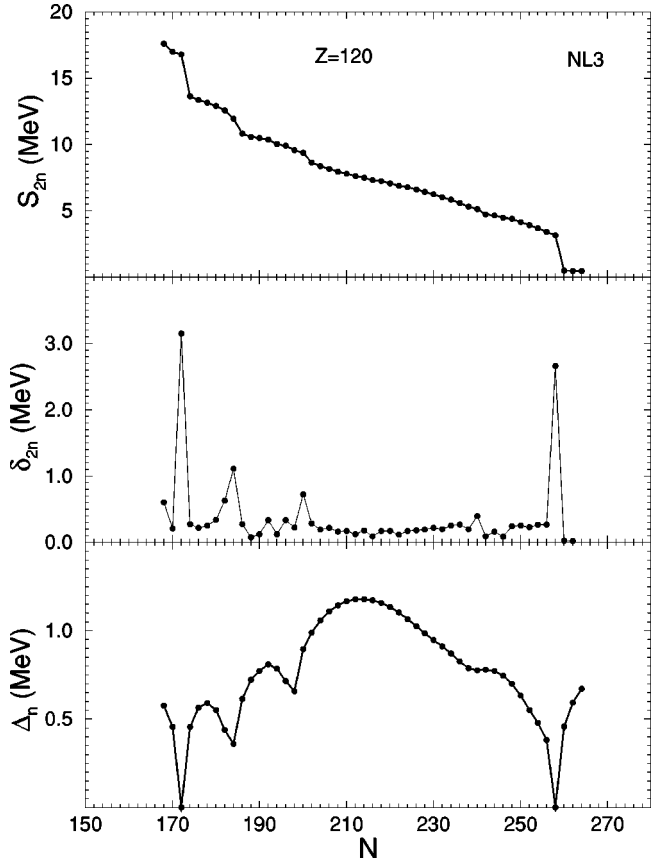

FIG. 3. Same as Fig. 1 but for the relativistic parameter set NL3.

particle levels for the neutron numbers corresponding to the shell closures detected above. Let us now look into the neutron single-particle spectra, displayed in Fig. 4, for the $^{292}120$, $^{304}120$, and $^{378}120$ nuclei. All the three parameter sets G2, G1, and NL3 show a large gap above the Fermi energy for $N=172$ and 258. But for the neutron number $N=184$, there appear only moderate gaps across the Fermi level for the G2 and G1 sets, and the gap is still smaller for NL3. This is in agreement with our previous discussions of the other indicators.

Inspecting the $N=258$ level spectrum one can appreciate another visible energy gap across the neutron numbers $N=228$ ($1k_{17/2}$ level) and $N=198$ ($1j_{13/2}$ level) in all of the parameter sets. In spite of this, no distinct indications for a shell closure were found for $N=228$ or $N=198$ in the curves of S_{2n}, δ_{2n}, and Δ_n in Figs. 1–3. If one compares the spectra for the three systems $N=172$, 184, and 258, it can be noted that the gap between two particular levels is strongly modified along the isotopic chain. Consequently, an analysis of the spectra alone would not suffice and the use of the discussed energy indicators becomes mandatory in order to make predictions for shell closures in superheavy nuclei.

B. Isotonic chains

We now proceed to discuss the isotonic chains of the neutron numbers which we have detected as candidates for spherical shell closures in the preceding study of the isotopic chain of $Z=120$. We start with the $N=172$ isotonic chain in Fig. 5, which displays the two-proton separation energy S_{2p}, the two-proton shell gap δ_{2p}, and the average pairing gaps Δ_p and Δ_n in the superheavy region from $Z=100$ up to the proton drip line, for the EFT model G2 and for the conventional RMF model NL3. For brevity we do not present the results from the G1 set, since the preceding section has shown that the predictions of G2 differ from NL3 more than in the case of G1.

From Fig. 5 one realizes that all the indicators signal a very robust shell closure at $Z=120$, and a much weaker shell closure at $Z=114$. The proton gap δ_{2p} ($\sim$5 MeV) of the nucleus $^{292}120$ is nearly twice as large as the corresponding neutron gap δ_{2n} ($\sim$3 MeV, Figs. 1 and 3). For the NL3 set, in addition, a little jump in S_{2p} and a small peaked structure in δ_{2p} indicates the possibility of a weak shell closure taking place at $Z=106$. It is nevertheless known that the region around $Z=106$ is deformed [36] and thus the spherical solution does not correspond to the ground state. Moreover, from the bottom panel of Fig. 5, we see that the neutron pairing

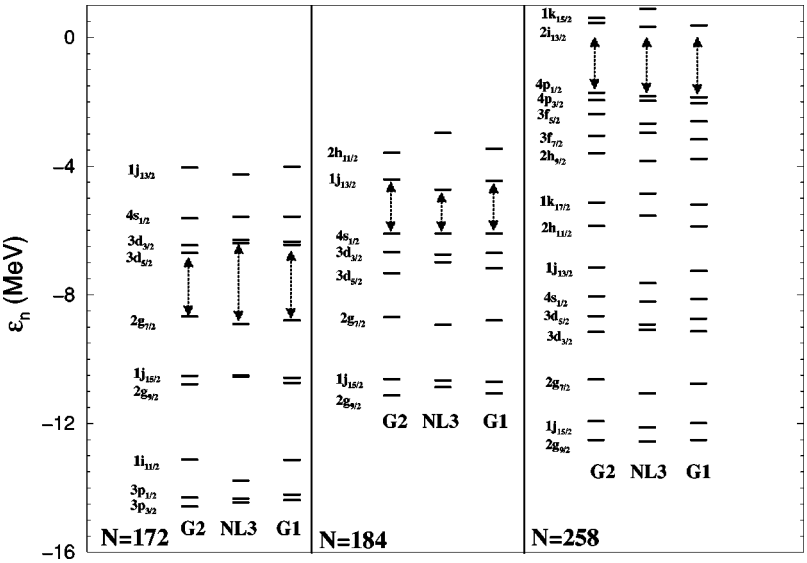

FIG. 4. Single-particle spectrum of neutrons in the vicinity of the Fermi level for the superheavy isotopes $^{292}120$, $^{304}120$, and $^{378}120$ computed with the relativistic interactions G1, G2, and NL3.

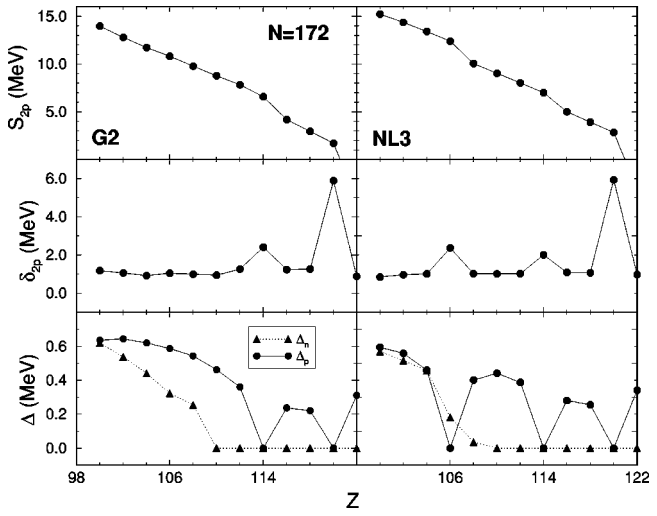

FIG. 5. The change with the proton number Z of the two-proton separation energy S_{2p}, the two-proton shell gap δ_{2p}, and the proton Δ_p and neutron Δ_n average pairing gaps for $N=172$ isotones obtained from spherical calculations with the relativistic parameter sets G2 (left panels) and NL3 (right panels).

gap Δ_n vanishes from $Z=110$ till the proton drip point, but it is nonzero for smaller atomic numbers. The nonvanishing neutron pairing gap for the $(N=172, Z=106)$ combination tells us that this cannot be a doubly closed shell nucleus. Therefore, the neutron number $N=172$ exhibits a strong shell closure for the proton number $Z=120$ but this magicity is washed out for $Z \leqslant 110$. In conclusion, in the region of superheavy nuclei the magicity of a particular neutron number depends on the number of protons present in the nucleus.

We next analyze the shell closures for $N=184$ and $N=258$ in combination with different proton numbers. In Fig. 6 we display the results for the $N=184$ isotonic chain. Curves are somewhat similar to those for $N=172$. In the G2 parametrization one identifies $Z=114$ and $Z=120$ as possible shell closures though the size of the jump in δ_{2p}, which is similar for both proton numbers, is small if we compare it

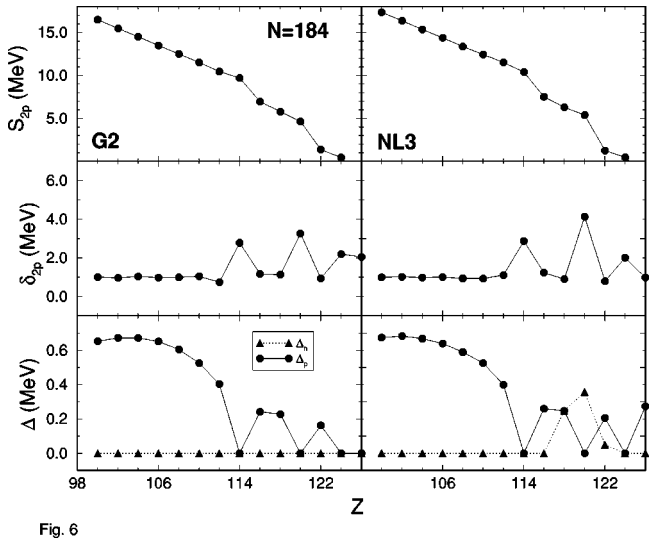

FIG. 6. Same as Fig. 5 but for the isotones of $N=184$.

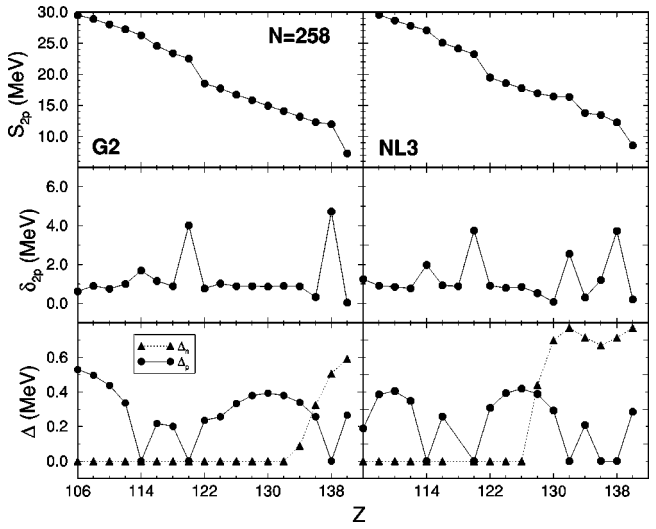

FIG. 7. Same as Fig. 5 but for the isotones of $N=258$.

with the jump observed for $(N=172, Z=120)$ in Fig. 5. In the case of the NL3 parameter set there is some evidence for a weak shell closure at $Z=114$ only, because the neutron pairing gap for $Z=120$ does not vanish which prevents the combination $(N=184, Z=120)$ from representing a doubly magic nucleus. The results for $N=258$ neutrons are shown in Fig. 7. We again find a strong signature for a shell closure at $Z=120$ in both the G2 and NL3 parameter sets, whereas the indications for a shell closure at $Z=114$ are much weaker. One also observes prominent jumps in S_{2p} and δ_{2p} at $Z=132$ (NL3) and $Z=138$ (NL3 and G2). But in this region, close to the proton drip line, the neutron pairing gap does not vanish. This implies that only the combination of $N=258$ with proton numbers $Z=114$ and $Z=120$ may exhibit a double shell closure character.

Figure 8 depicts the proton single-particle spectra obtained with the G2 and NL3 parametrizations for the illustrative examples of the $^{286}114$, $^{292}120$, $^{298}114$, and $^{304}120$ nuclei. Looking at the proton spectra for the systems with $N=172$, a very large gap can be observed for 120 protons (between the $2f_{5/2}$ and $3p_{3/2}$ levels for G2, and between the $2f_{5/2}$ and $1i_{11/2}$ levels for NL3). Instead, practically no gap exists for 114 protons (between the $2f_{7/2}$ and $2f_{5/2}$ levels), specially for the NL3 set. This is consistent with the very weak signals of magicity of $Z=114$ in the case of the $N=172$ isotonic chain shown by the S_{2p} and δ_{2p} indicators in Fig. 5.

With the addition of only 12 neutrons, the proton spectra for the systems with $N=184$ exhibit a different pattern than for $N=172$ near the Fermi energy (cf. Fig. 8). The gaps occurring between the levels corresponding to 114 protons and to 120 protons are now comparable in magnitude. This fact is in agreement with the relatively magic character of the $^{298}114$ and $^{304}120$ nuclei predicted by the indicators plotted in Fig. 6. In any case, even for $N=184$, the magicity of $Z=114$ is always smaller than the one shown by $Z=120$, as one can see from the comparison of S_{2p} and δ_{2p} in Figs. 5 and 6. This discussion shows again the strong dependence of the proton (neutron) shell closures of SHE on the neutron (proton) numbers and thus the importance of using the energy indicators.

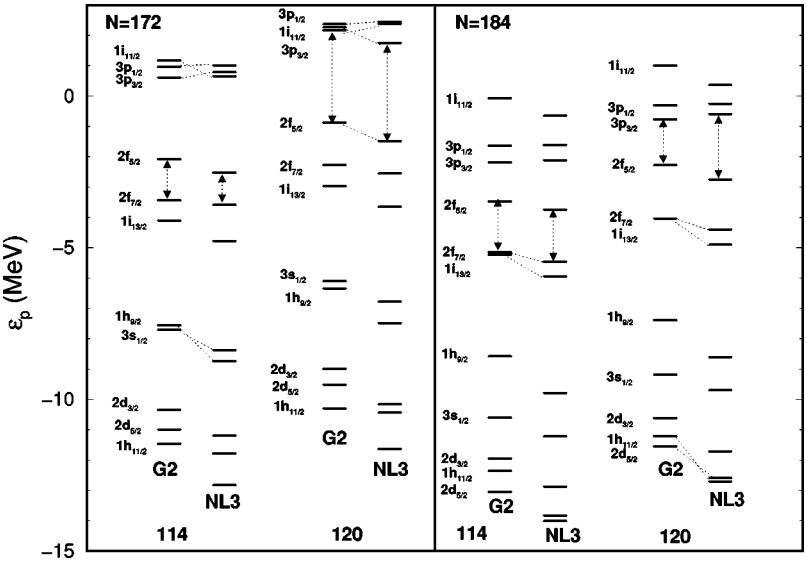

FIG. 8. Single-particle spectrum of protons in the vicinity of the Fermi level for the superheavy isotones $^{286}114$ and $^{292}120$ (left panel), and $^{298}114$ and $^{304}120$ (right panel) computed with the relativistic interactions G2 and NL3.

C. Shell corrections

The stability of superheavy elements with an atomic number larger than $Z\sim 100$ is possible thanks to the shell effects. In the liquid droplet model picture these superheavy nuclei are unstable against spontaneous fission because the large Coulomb repulsion can no longer be compensated by the nuclear surface tension. However, SHE may still exist because the quantal shell corrections generate local minima in the nuclear potential energy surface which provide additional stabilization.

In our context the shell correction energy is also useful as a different test for checking the robustness of the shell closures. For experimentally known shell closures, i.e., up to $Z=82$ and $N=126$, the shell corrections are strongly peaked around the magic numbers (see, e.g., Ref. [60]), providing enhanced binding for magic nuclei. However, in the superheavy mass region, instead of displaying sharp jumps, the shell corrections depict a landscape of rather broad areas of shell stabilized nuclei [34,36]. Still, in these areas the closed shell nuclei show a larger stabilization (i.e., more negative shell corrections) than their neighbors. In the present section we want to study the shell corrections around our selected nuclei with $Z=114$ and $Z=120$, and $N=172$, 184, and 258.

The calculation of the shell correction energy is based on the Strutinsky energy theorem [61] which states that the total quantal energy can be divided in two parts:

$$E=\tilde{E}+E_{\mathrm{shell}}. \tag{4}$$

The largest piece $\tilde{E}$ is the average part of the energy which depends in a smooth way on the number of nucleons (namely, the part well represented by the liquid droplet model). The smaller piece, the shell correction E_{shell}, has instead an oscillating behavior. The oscillations are due to the grouping of levels into shells and display maxima at the shell closures. According to the idea of Strutinsky, the average part of the ground-state energy of a shell model potential can be obtained by replacing the Hartree-Fock occupation numbers n_α (1 or 0 for occupied or empty states) with occupation numbers $\tilde{n}_\alpha$ smoothed by an averaging function [59]. The shell correction E_{shell} is computed as the difference of the exact energy to that average part.

The Strutinsky smoothing procedure requires the use of several major shells. This faces the problem of the treatment of the continuum when realistic finite depth potentials are employed [34,36,62,63]. Our strategy here, working in coordinate space, and consistently with our approach to the treatment of pairing, is to perform the Strutinsky smoothing including the quasibound levels which are retained by their centrifugal barrier (centrifugal-plus-Coulomb barrier for protons). We have taken seven major shells above the Fermi energy (i.e., states up to around 50 MeV above the Fermi level) and have considered curvature corrections up to $2M=10$ [59]. We have found that the plateau condition of the averaged energy [59] is fulfilled for a smoothing parameter $\gamma\sim 1.3-1.6$ MeV for both protons and neutrons. As we have discussed, the quasibound levels included in our calculation do not depend on the size of the box where the calculation is performed. These levels, usually with high angular momentum, lie close in energy to the RHB canonical levels [46]. Of course, one limitation of our approach is that some resonant levels with low angular momentum can be missed, more easily for neutrons, and then their contribution is shared among the higher angular momentum levels which we include in the calculation.

The total (neutron-plus-proton) shell corrections stemming from our calculations for the isotopic chains with $Z=114$ and $Z=120$ are displayed in Fig. 9. The equivalent graph for the isotonic chains with $N=172$, 184, and 258 is presented in Fig. 10. Again, we point out that our calculation is performed in spherical symmetry and thus the calculated shell corrections represent in general an upper bound to the actual ones. Stronger shell stabilization could still be provided by deformation. The magnitude of the shell correction energy E_{shell} is dictated by the level density around the Fermi level. A high level density in the vicinity of the Fermi energy yields a positive shell correction reducing the binding energy, whereas a low level density gives a negative shell correction which increases the binding energy. The shell correc-

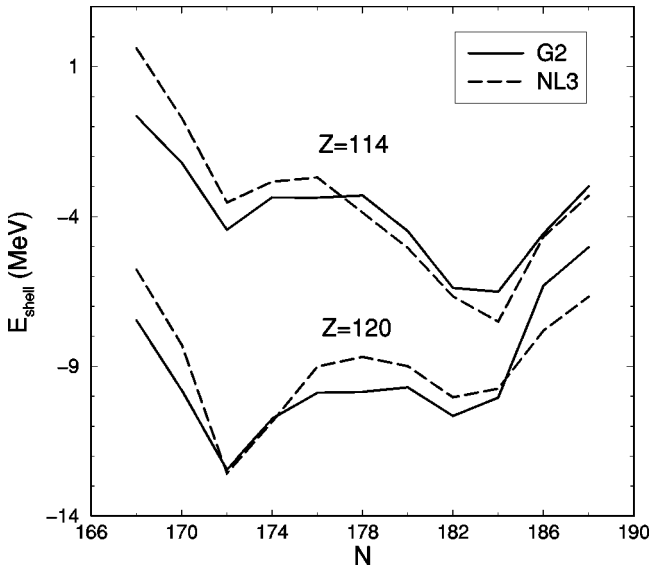

FIG. 9. The change of the total shell correction energy (sum of the neutron and proton contributions) with the neutron number N for the isotopes of $Z=114$ and $Z=120$ in spherical calculations with the G2 and NL3 models.

tions obtained with the G2 and NL3 sets are rather similar for the investigated isotopic and isotonic chains. This is so because the single-particle levels around the Fermi surface essentially show the same ordering with both parameter sets and there are only small differences in the spin-orbit splittings, as it can be realized from Figs. 4 and 8. The results for the set G1 are also similar to those of G2 and NL3 and thus we do not display them in Figs. 9 and 10.

In Fig. 9 the isotopic chain of $Z=120$ shows a large negative shell correction at $N=172$, due to the presence of low angular momentum levels near the Fermi energy for both neutrons ($4s_{1/2}$, $3d_{3/2}$, and $3d_{5/2}$ levels) and protons ($3p_{1/2}$ and $3p_{3/2}$ levels). These levels imply a comparatively lower level density and thus a more negative shell correction. The isotopic chain also shows another local minimum around $N=182-184$, but in this case the shell correction energy is less negative than for $N=172$. The pattern exhibited by the total shell correction for the $Z=120$ isotopes looks very similar to that of the neutron shell correction displayed in Fig. 5 of Ref. [34] for the NL3 parameter set, which was computed by means of the Green's function procedure. Looking at the curves for the $Z=114$ isotopic chain represented in Fig. 9 one realizes that the shell corrections are globally weaker than that for $Z=120$ chain, which means less stability. They also present minima at $N=172$ and at $N=184$, although in this case the situation is reversed and the largest corrections correspond to $N=184$ instead of $N=172$.

In the upper panel of Fig. 10 the shell corrections for the $N=172$ isotonic chain clearly show only one minimum at $Z=120$. The $N=184$ chain (middle panel) displays one more local minimum at $Z=114$, though the magnitude of the shell correction obtained for $Z=114$ is smaller than for $Z=120$. Our total shell corrections for $N=172$ and $N=184$ show similar patterns to the proton shell corrections of NL3 which are depicted in Fig. 6 of Ref. [34] for these same isotonic chains. The curves of the shell correction for the $N=258$ hyperheavy nuclei (lower panel of Fig. 10) are overall very much flat in comparison to those for the isotonic chains of $N=172$ and $N=184$. The absolute minimum again appears at $Z=120$. There is also a very small kink at $Z=114$. The comparison of the curves in the three panels reveals that at $Z=120$ all the curves show the most prominent minima. At $Z=114$, the shell corrections for $N=172$ have no dip at all, but they display a small kink for $N=184$ and $N=258$.

From the analysis of the shell correction energy we see that the location of the minima in the shell stabilized regions of SHE is in good agreement with the conclusions about the shell closures that we inferred from the study of the previous indicators. Due to the fact that the minima in the shell corrections for superheavy nuclei are often not very pronounced, but rather shallow, we note the usefulness of analyzing the shell corrections as a complementary means to assess the predictions made on the basis of the energy indicators.

IV. SUMMARY AND CONCLUSIONS

We have investigated the predictions of the G1 and G2 parametrizations of Ref. [38] obtained from the modern effective field theory approach to relativistic nuclear phenomenology for the occurrence of spherical double shell closures

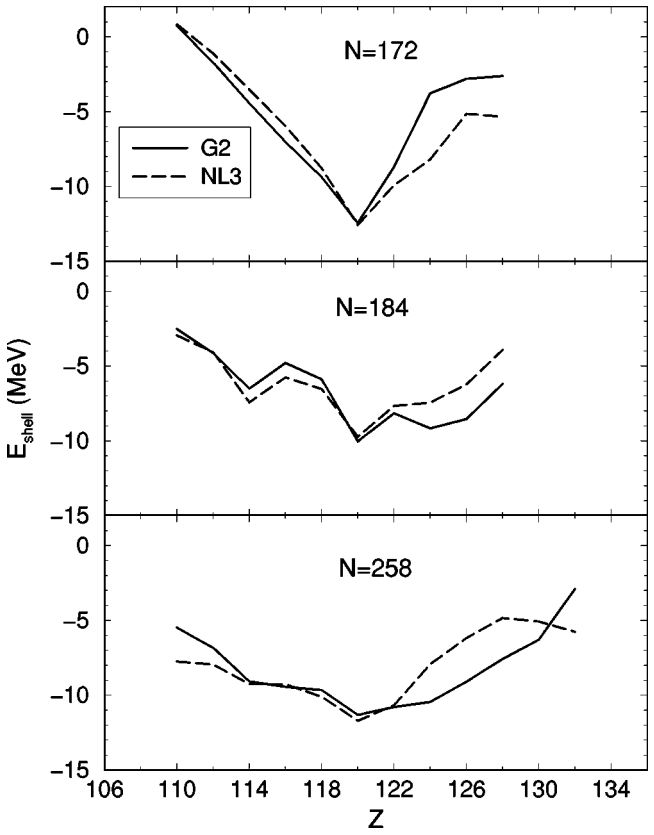

FIG. 10. The change of the total shell correction energy (sum of the neutron and proton contributions) with the proton number Z for the isotonic chains of $N=172$, $N=184$, and $N=258$ neutrons in spherical calculations with the G2 and NL3 models.

and the shell stabilizing effect in superheavy nuclei. Within an isotopic or isotonic chain of SHE the possible shell closures are identified by a simultaneous occurrence at a given Z or N of a large jump in the corresponding two-nucleon separation energy S_{2q}, a pronounced peak in the two-nucleon shell gap δ_{2q}, and the vanishing of the average pairing gaps Δ_n and Δ_p. To treat the pairing correlations we have employed an improved BCS model that was used successfully in Ref. [46] in calculations of isotopic and isotonic chains with magic proton or neutron numbers.

First we have studied the isotopic chain of $Z=120$, which is found to be a magic number in previous RMF calculations. Neutron shell closures arise at $N=172$ and $N=258$ in all the considered parameter sets (G1, G2, and NL3). In the particular case of the G2 set $N=184$ appears as another possible neutron shell closure, though it is not as robust as for $N=172$ or $N=258$. The magic character of $Z=120$ is supported by the fact that the average proton pairing gap vanishes along the whole isotopic chain. Next we have investigated the isotonic chains with $N=172$, 184, and 258 for $Z>100$. From this analysis the candidates to proton shell closures have been found to be $Z=114$ (weakly) and $Z=120$ (strongly). Other possible candidates different from $Z=114$ and $Z=120$ present a nonvanishing neutron pairing gap. We conclude that the parameter sets G1 and G2 derived from the effective field theory approach clearly point out towards the doubly magic character of the $(N=172, Z=120)$ and $(N=258, Z=120)$ combinations, which is in agreement with the predictions of the NL3 set.

A minimum condition for a superheavy nucleus to be stable against fission is that the shell effects must be able to provide enough binding to compensate for the huge Coulomb repulsion among protons. Compared to normal nuclei where the large negative shell corrections are peaked at the magic numbers, the SHE display broad areas of shell stabilization around the possible shell closures. We have computed the shell corrections for the analyzed superheavy nuclei by means of an Strutinsky smoothing. The continuum has been parametrized by taking quasibound levels which in coordinate space are retained by their centrifugal barrier.

We have found a region of shell stabilization for isotopes of $Z=114$ and $Z=120$ in the range of neutron numbers $N\sim 170-186$. The shell corrections are larger for $Z=120$ than for $Z=114$, and in both cases show peaks at $N=172$ and $N=184$ which indicates the larger stability of these nuclei relative to their neighbors. For the isotonic chains of $N=172$ and $N=184$ the more negative shell corrections appear at $Z=120$, although a smaller peak shows up at $Z=114$ pointing out the relatively stable character of this nucleus, at least compared with the immediate neighbors. The curve of the shell corrections for the isotones of $N=258$ is mostly flat, but again a depression can be recognized around $Z=120$.

To summarize, in previous works [45,46] we showed that the parameter sets derived from the effective field theory approach to the low-energy nuclear many-body problem [38] work nicely for both β-stable and β-unstable nuclei. This is in addition to their ability to yield a realistic equation of state at densities above saturation which compares very favorably with microscopic Dirac-Brueckner-Hartree-Fock calculations [45]. In the present study we have applied the EFT model to deal with the theoretical description of some properties of superheavy nuclei. In particular, we have seen that the G1 and G2 parameter sets reproduce the strong double shell closure at $N=172$ and $Z=120$ predicted by the standard RMF parametrizations, as well as a double shell closure at $N=258$ and $Z=120$. Interestingly enough, the new parameter set G2 shows some evidence for a double shell closure of the $N=184$, $Z=114$ nucleus traditionally predicted by the macroscopic-microscopic models, as well as by the Skyrme interaction SkI4.

The results presented here are a first prospect of the performance of the EFT model in the description of SHE. Our calculations have been restricted to spherical shapes. As we have discussed, this is not an impeding drawback for the effects investigated in this work. However, for comparisons with the measured data on the heavier actinides and the experimentally synthesized SHE around $Z=110$, one definitively needs to perform deformed calculations. In future it will be worthwhile trying to include deformation degrees of freedom into the EFT model to extend the study to deformed nuclei of the SHE island.

ACKNOWLEDGMENTS

Two of us (X.V. and M.C.) acknowledge financial support from the DGI (Ministerio de Ciencia y Tecnología, Spain) and FEDER under Grant No. BFM2002-01868 and from DGR (Catalonia) under Grant No. 2001SGR-00064. T.S. thanks the Spanish Education Ministry Grant No. SB2000-0411 for financial support and the Departament d'Estructura i Constituents de la Matèria of the University of Barcelona for kind hospitality.

[1] S. Hofmann, Rep. Prog. Phys. **61**, 639 (1998); Eur. Phys. J. A **15**, 195 (2002).
[2] S. Hofmann and G. Münzenberg, Rev. Mod. Phys. **72**, 733 (2000).
[3] P. Armbruster, Annu. Rev. Nucl. Part. Sci. **50**, 411 (2000).
[4] P. Möller and J. R. Nix, Nucl. Phys. **A549**, 84 (1992); J. Phys. G **20**, 1681 (1994).
[5] R. Smolańczuk, Phys. Rev. C **56**, 812 (1997).
[6] T. Bürvenich, K. Rutz, M. Bender, P.-G. Reinhard, J. A. Maruhn, and W. Greiner, Eur. Phys. J. A **3**, 139 (1998).
[7] Yu. Ts. Oganessian *et al.*, Eur. Phys. J. A **5**, 63 (1999); Nature (London) **400**, 242 (1999); Eur. Phys. J. A **15**, 201 (2002).
[8] W. D. Myers and W. J. Swiatecki, Nucl. Phys. **A81**, 1 (1966).
[9] A. Sobiczewski, F. A. Gareev, and B. N. Kalinkin, Phys. Lett. **22**, 500 (1966).
[10] S. G. Nilsson *et al.*, Nucl. Phys. **A115**, 545 (1968).
[11] U. Mosel and W. Greiner, Z. Phys. **222**, 261 (1969).
[12] S. Ćwiok, W. Nazarewicz, and P. H. Heenen, Phys. Rev. Lett.

83, 1108 (1999).
[13] M. Bender, Phys. Rev. C **61**, 031302 (2000).
[14] S. K. Patra, W. Greiner, and R. K. Gupta, J. Phys. G **26**, L65 (2000).
[15] A. Mamdouh, J. M. Pearson, M. Rayet, and F. Tondeur, Nucl. Phys. **A679**, 337 (2001).
[16] Zhongzhou Ren and H. Toki, Nucl. Phys. **A689**, 691 (2001).
[17] Zhongzhou Ren, Phys. Rev. C **65**, 051304 (2002).
[18] Zhongzhou Ren, Fei Tai, and Ding-Han Chen, Phys. Rev. C **66**, 064306 (2002).
[19] Zhongzhou Ren, Ding-Han Chen, Fei Tai, H. Y. Zhang, and W. Q. Shen, Phys. Rev. C **67**, 064302 (2003).
[20] W. Nazarewicz, M. Bender, S. Ćwiok, P. H. Heenen, A. T. Kruppa, P.-G. Reinhard, and T. Vertse, Nucl. Phys. **A701**, 165 (2002).
[21] A. V. Afanasjev, T. L. Khoo, S. Frauendorf, G. A. Lalazissis, and I. Ahmad, Phys. Rev. C **67**, 024309 (2003).
[22] S. Typel and B. A. Brown, Phys. Rev. C **67**, 034313 (2003).
[23] M. Bender, P. Bonche, T. Duguet, and P.-H. Heenen, Nucl. Phys. **A723**, 354 (2003).
[24] Y. K. Gambhir, A. Bhagwat, M. Gupta, and A. K. Jain, Phys. Rev. C **68**, 044316 (2003).
[25] T. Bürvenich, M. Bender, J. A. Maruhn, and P.-G. Reinhard, Phys. Rev. C **66**, 014307 (2004).
[26] S. Goriely, M. Samyn, P.-H. Heenen, J. M. Pearson, and F. Tondeur, Phys. Rev. C **66**, 024326 (2002).
[27] S. Ćwiok, J. Dobaczewski, P.-H. Heenen, P. Magierski, and W. Nazarewicz, Nucl. Phys. **A611**, 211 (1996).
[28] M. Bender, K. Rutz, P.-G. Reinhard, J. A. Maruhn, and W. Greiner, Phys. Rev. C **58**, 2126 (1998).
[29] D. Hirata, K. Sumiyoshi, B. V. Carlson, H. Toki, and I. Tanihata, Nucl. Phys. **A609**, 131 (1996).
[30] J.-F. Berger, L. Bitaud, J. Dechargé, M. Girod, and K. Dietrich, Nucl. Phys. **A685**, 1 (2001).
[31] J. Dechargé, J.-F. Berger, M. Girod, and K. Dietrich, Nucl. Phys. **A716**, 55 (2003).
[32] K. Rutz, M. Bender, T. Bürvenich, T. Schilling, P.-G. Reinhard, J. A. Maruhn, and W. Greiner, Phys. Rev. C **56**, 238 (1997).
[33] M. Bender, K. Rutz, P.-G. Reinhard, J. A. Maruhn, and W. Greiner, Phys. Rev. C **60**, 034304 (1999).
[34] A. T. Kruppa, M. Bender, W. Nazarewicz, P.-G. Reinhard, T. Vertse, and S. Ćwiok, Phys. Rev. C **61**, 034313 (2000).
[35] P.-G. Reinhard, M. Bender, and J. A. Maruhn, Comments Mod. Phys., Part C **2**, A177 (2002).
[36] M. Bender, W. Nazarewicz, and P.-G. Reinhard, Phys. Lett. B **515**, 42 (2001).
[37] R. J. Furnstahl, B. D. Serot, and H. B. Tang, Nucl. Phys. **A598**, 539 (1996).
[38] R. J. Furnstahl, B. D. Serot, and H. B. Tang, Nucl. Phys. **A615**, 441 (1997); **A640**, 505 (1998).
[39] B. D. Serot and J. D. Walecka, Int. J. Mod. Phys. E **6**, 515 (1997).
[40] C. Speicher, R. M. Dreizler, and E. Engel, Ann. Phys. (N.Y.) **213**, 312 (1992).
[41] R. J. Furnstahl and B. D. Serot, Nucl. Phys. **A671**, 447 (2000).
[42] B. D. Serot and J. D. Walecka, Adv. Nucl. Phys. **16**, 1 (1986).
[43] J. Boguta and A. R. Bodmer, Nucl. Phys. **A292**, 413 (1977).
[44] M. Del Estal, M. Centelles, and X. Viñas Nucl. Phys. **A650**, 443 (1999).
[45] M. Del Estal, M. Centelles, X. Viñas, and S. K. Patra, Phys. Rev. C **63**, 024314 (2001); M. Centelles, M. Del Estal, X. Viñas, and S. K. Patra, in *The Nuclear Many-Body Problem 2001*, Vol. 53 of NATO Advanced Studies Institute Series B: Physics, edited by W. Nazarewicz and D. Vretenar (Kluwer, Dordrecht, 2002), p. 97.
[46] M. Del Estal, M. Centelles, X. Viñas, and S. K. Patra, Phys. Rev. C **63**, 044321 (2001).
[47] M. A. Huertas, Phys. Rev. C **66**, 024318 (2002).
[48] G. A. Lalazissis, J. König, and P. Ring, Phys. Rev. C **55**, 540 (1997).
[49] J. J. Rusnak and R. J. Furnstahl, Nucl. Phys. **A627**, 495 (1997).
[50] R. J. Furnstahl, J. J. Rusnak, and B. D. Serot, Nucl. Phys. **A632**, 607 (1998).
[51] J. Dobaczewski, H. Flocard, and J. Treiner, Nucl. Phys. **A422**, 103 (1984); J. Dobaczewski, W. Nazarewicz, T. R. Werner, J.-F. Berger, R. C. Chin, and J. Dechargé, Phys. Rev. C **53**, 2809 (1996).
[52] J. Dechargé, and D. Gogny, Phys. Rev. C **21**, 1568 (1980).
[53] J. Meng, Phys. Rev. C **57**, 1229 (1998); Nucl. Phys. **A635**, 3 (1998).
[54] J. Meng and I. Tanihata, Nucl. Phys. **A650**, 176 (1999).
[55] G. A. Lalazissis, D. Vretenar, and P. Ring, Phys. Rev. C **57**, 2294 (1998).
[56] D. Vretenar, G. A. Lalazissis, and P. Ring, Phys. Rev. C **57**, 3071 (1998).
[57] G. A. Lalazissis, M. M. Sharma, P. Ring, and Y. K. Gambhir, Nucl. Phys. **A608**, 202 (1996).
[58] E. Chabanat, P. Bonche, P. Haensel, J. Meyer, and R. Schaeffer, Nucl. Phys. **A635**, 231 (1998).
[59] P. Ring and P. Schuck, *The Nuclear Many-Body Problem* (Springer-Verlag, Berlin, 1980).
[60] M. Kleban, B. Nerlo-Pomorska, J. F. Berger, J. Dechargé, M. Girod, and S. Hilaire, Phys. Rev. C **65**, 024309 (2002); B. Nerlo-Pomorska, K. Pomorski, J. Bartel, and K. Dietrich, *ibid.* **66**, 051302 (2002).
[61] V. M. Strutinsky, Nucl. Phys. **A122**, 1 (1968); Nucl. Phys. **A218**, 169 (1974).
[62] M. Bolsterli, E. O. Fiset, J. R. Nix, and J. L. Norton, Phys. Rev. C **5**, 1050 (1972).
[63] W. Nazarewicz, T. R. Werner, and J. Dobaczewski, Phys. Rev. C **50**, 2860 (1994); T. Vertse, A. T. Kruppa, R. J. Liotta, W. Nazarewicz, N. Sandulescu, and T. R. Werner, *ibid.* **57**, 3089 (1998).